nDEP microwells for single-cell patterning in physiological media†

Nikhil Mittal,‡[a] Adam Rosenthal‡[bc] and Joel Voldman*[b]

Received 26th April 2007, Accepted 21st June 2007
First published as an Advance Article on the web 10th July 2007
DOI: 10.1039/b706342c

We present a novel technique to accurately position single cells on a substrate using negative dielectrophoresis and cell–substrate adhesion. The cells are suspended in physiological media throughout the patterning process. We also verify the biocompatibility of this method by demonstrating that the patterned cells proliferate and show normal morphology. We calculate the temperatures and transmembrane potential that cells in the device experience and compare them to physiologically acceptable levels described in previous studies.

Introduction

The ability to place cells at specific locations on a substrate is a useful tool for studying and engineering interactions between cells,[1–5] performing image-based cell selection,[6,7] and creating cell-based biosensors.[8,9] The ability to pattern with single-cell resolution is necessary in order to perform studies of single-cell physiology in which these cells are interacting with other cells. For example, such technology would enable the precise construction and study of neuronal networks,[10] and *in vitro* studies of interactions between stem cells and surrounding niche cells that control their division.[11] For example, in the Drosophila germarium, germline stem cells are found in direct contact with cap cells.

Several techniques have been used for creating patterns of mostly single cells: (i) patterning the substrate with materials that support and/or resist cell adhesion,[12,13] sometimes with the additional use of electrophoretic forces,[6,14] (ii) loading cells into microwells[15] or trapping structures,[16] (iii) using positive dielectrophoretic (pDEP) forces[2,7,17–20] to pull cells onto patterned electrodes, (iv) negative dielectrophoretic (nDEP) forces[21–23] to push cells (for a review see Voldman[24]), (v) cell stamping,[25] and (vi) laser printing.[26] Among these techniques, electrical approaches to patterning have the beneficial feature that they do not restrict subsequent cell proliferation or motility (Fig. 1). Another advantage of electrical methods is that they enable electrical addressing of sites where cells are held,[7] allowing for the easy integration of electrical detection of cell products and/or electrical stimulation of particular cells.

While pDEP-based cell patterning has become increasingly popular over the last few years,[2,7,17–20] there have been fewer studies that used nDEP to pattern cells.[21–23] This is predominantly because nDEP traps are weaker and harder to design, since, unlike pDEP, particles are trapped at electric field minima. However, in contrast to pDEP, which must be performed in media with low conductivity to guarantee that the cells are more polarizable than the media, *only* nDEP can be performed with cells suspended in commonly used cell-culture media because these media have higher conductivity and relative permittivity than cells[27,28] (ESI†). The use of such media presents a significant advantage because it allows one to use the traditional media formulations optimized for cell culture. This avoids any gross viability issues associated with placing sensitive cells in artificial media (ESI†).

Previously we demonstrated the use of nDEP forces to construct traps that were used to hold single micron-size *beads*

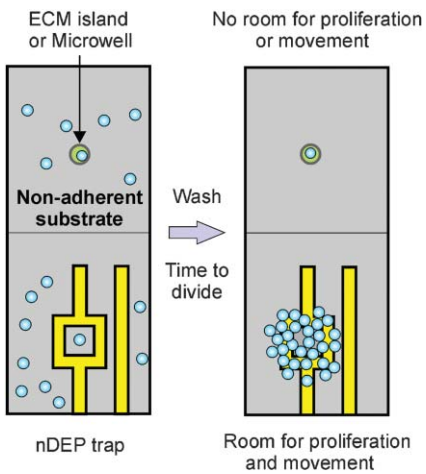

Fig. 1 The use of DEP-based single-cell patterning for patterning proliferating and/or migrating cells. Adhesive patterning of the extracellular matrix (ECM) or patterning using PDMS structures such as microwells cannot provide room for proliferation or movement while patterning single cells. Using single-cell nDEP traps it is possible to both trap single cells and provide room for proliferation and movement.

[a]*Department of Physics, Massachusetts Institute of Technology, Cambridge, MA, 02139, USA*
[b]*Department of Electrical Engineering and Computer Science, Massachusetts Institute of Technology, Cambridge, MA, 02139, USA. E-mail: voldman@mit.edu; Fax: +1-617-258-5846; Tel: +1-617-324-1423*
[c]*Harvard-MIT Division of Health Science and Technology, Massachusetts Institute of Technology, Cambridge, MA, 02139, USA*

† Electronic supplementary information (ESI) available: Cells in cell-culture media only experience negative dielectrophoresis; cell–substrate friction/sticking and nDEP microwell design motivation; effect of cell size and shape on the levitation height; operating voltages; temperature modeling and measurements; EHD voltage estimation; effects of low-conductivity (pDEP) media on ES cells; angle of flow; video clip showing manipulation of cells in our device. See DOI: 10.1039/b706342c

‡ These authors contributed equally to this work.

at chosen locations on a substrate.[29] Here we present modifications to that design that allow us to manipulate and pattern single *cells*. This required adding interdigitated electrodes to minimize non-specific cell adhesion and determining operating parameters that minimized heating and electric field exposure. The resulting structures are termed nDEP microwells to reflect the fact that they present an electrical microwell to incoming cells, allowing cell–substrate attachment only inside the DEP trap. Unlike nDEP-based structures developed by other groups,[22,23] our nDEP microwells are accurately sized so as to allow only single cells to settle on the substrate. We demonstrate that our cell-patterning technique does not affect gross cell phenotype as measured by morphology and proliferation. Finally, we show how combining pressure-driven and convective flows can be used to manipulate cells in two dimensions.

Results

Evolution of the nDEP microwell

We previously demonstrated the use of nDEP forces to construct traps that were used to hold single micron-size beads at chosen locations on a substrate.[29] These traps employed a unique geometry consisting of a square electrode and a line-shaped counter-electrode (Fig. 2(a), inset). By appropriately sizing the square and the spacing between the square and the line, we could alter both the strength of the trap and its size selectivity. The resulting traps were strong, easy to fabricate, and optimally suited for particles in the size range of cells.

There were several challenges that we needed to address to use these traps with cells, specifically minimizing nonspecific adhesion and mitigating any effects on cell physiology. Nonspecific adhesion refers to the all-too-common phenomenon whereby cells attach to the substrate in undesired areas through nonspecific mechanisms such as hydrophobic interactions. This can result in poor patterning fidelity because cells will end up not only in the traps but in other areas as well (ESI†). When using adhesive patterning, the attachment of cells in certain regions is minimized by coating these regions with an inert surface such as polyethylene glycol.[12] We wanted to avoid this approach for two reasons. First, we wanted to develop a matrix-independent patterning technique (Fig. 1). Second, while PEGs prevent cell attachment (spreading), a frictional/adhesive force between a cell and the (coated) substrate it is on is, nevertheless, always present. This force is easily overcome in conventional cell patterning, where one washes cells away using pipettes and macroscopic flows. In our microfluidic systems with DEP traps, we apply relatively small forces to avoid ejecting cells from the trap, which may not be large enough to sweep away nonspecifically adhered cells. For instance, our quantitative models of the nDEP microwells yield DEP holding forces for cells in these traps of $\sim$1 pN (at 1 V_{PP}).

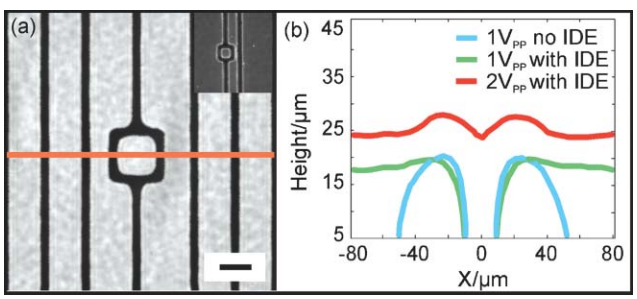

Fig. 2 nDEP microwell. (a) Image of an nDEP trap (center) surrounded by IDEs. Together they constitute a single nDEP microwell. The inset shows an nDEP trap without IDEs. The scale bar represents 20 μm. (b) Simulated equilibrium height of a cell in the device at positions along the orange line in a) for a substrate without IDEs (1 V_{pp}), and for a substrate with IDEs at 1 V_{pp} and 2 V_{pp}. Without IDEs, cells can contact the surface starting $\sim$50 μm from the trap. With IDEs, a well-like structure is formed at voltages of $\sim$1 V_{pp} as a result of levitation of cells by the IDEs, and the exclusion of fields inside the trap. The trap size is chosen so that only one cell can enter the nDEP microwell. As the voltage is increased, the well gets narrower, and finally "closes off" at 2 V_{pp}. The levitation of untrapped cells addresses the challenge of them sticking to the substrate (which impairs patterning).

We used a parallel-plate flow chamber with variable flow to estimate the frictional/adhesive forces holding cells on glass substrates. By using flow to release cells sticking to the surface, we estimated that this frictional force between the cell and the glass substrate ranges from 0.25–20 pN for HeLa cells and 10–25 pN for NIH 3T3 fibroblasts. This variation in the frictional force is greater than the DEP force exerted on trapped cells for physiologically acceptable voltages (see ESI† for details). Thus, effective patterning of cells in our device required that we prevent cell–substrate contact from occurring.

We decided to address this challenge by exploiting the capabilities of nDEP to prevent cell–substrate contact. We introduced interdigitated electrodes (IDEs) around the traps, which we used to levitate untrapped cells (Fig. 2(a)). The IDEs produce an nDEP force that is predominantly upward-directed, with minimal in-plane components. Thus, the IDEs only present a surface-repelling force but do not prevent the lateral movement of the cells. We chose an electrode spacing of 30 μm for our IDEs. Our simulations show an average equilibrium cell height of around 17 μm for this electrode spacing when the electrodes are actuated at 1 V_{pp} (Fig. 2(b), ESI†), which was consistent with our measurements. Since cell "radii" are typically around 5–8 μm, we surmised that this design would be sufficient to levitate cells. Our choice of electrode spacing was based on an inter-trap spacing of 200 μm, but our modeling software predicts that the levitation height is fairly insensitive to the electrode spacing for spacings in the range of 20–35 μm. However, as described in Rosenthal and Voldman,[29] the trap strength decreases strongly with increases in the spacing between the three central trap electrodes. For ease of fabrication, we chose this spacing to be 10 μm.

The combination of the nDEP trap and IDEs constitutes the nDEP microwell. In Fig. 3 we demonstrate patterning of single HL60 cells in these nDEP microwells. In about 30–60 minutes we could load cells into our device, direct cells into most traps (>70% of a total of 100 traps), and clear away untrapped cells. We see that the addition of the IDEs enables patterning with very little adhesion of cells outside the patterns (typically less than 10 cells per 100 trapped cells). When working with adherent cells it was possible to move the devices into an

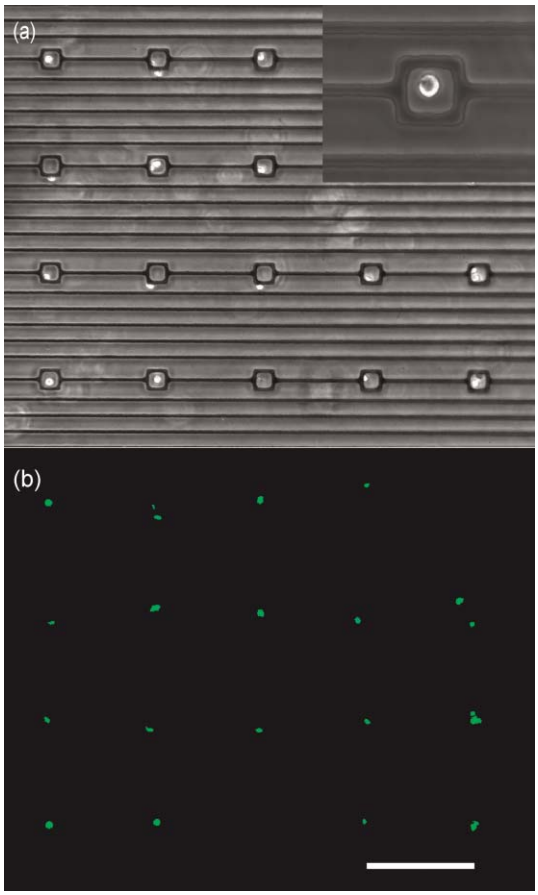

Fig. 3 Phase contrast (a) and fluorescence (b) images of HL60 cells trapped on our electrode array. Inset: Phase contrast image of a single trapped cell. The scale bar is 200 μm.

incubator after allowing the cells to attach for around 30 minutes. Non-adherent cells shifted from their positions on moving the device and consequently would have to be incubated on the microscope stage for longer assays.

Cell health

The second question that must be addressed when using cells in any DEP-based device is whether the DEP manipulation affects cell physiology. Two mechanisms have been described by which alternating electric fields can affect normal cell physiology,[17,27] namely, Joule heating of the cell suspension, and induction of large transmembrane potentials ultimately leading to electro-poration of the plasma membrane[30] or the membranes of intracellular organelles.[31] In order to demonstrate that our trapping method is biocompatible, we designed the device to operate well beneath the damage thresholds associated with the mechanisms mentioned above. We excluded any investigation of damage to intracellular structures since the fields responsible for these effects have been reported to be two orders of magnitude higher than the fields in our device.[31]

To avoid any harmful effects due to Joule heating, we wanted to avoid temperature excursions above physiological levels (37 °C for mammalian cells). We simulated the temperatures experienced by cells at various voltages (Fig. 4(a)).

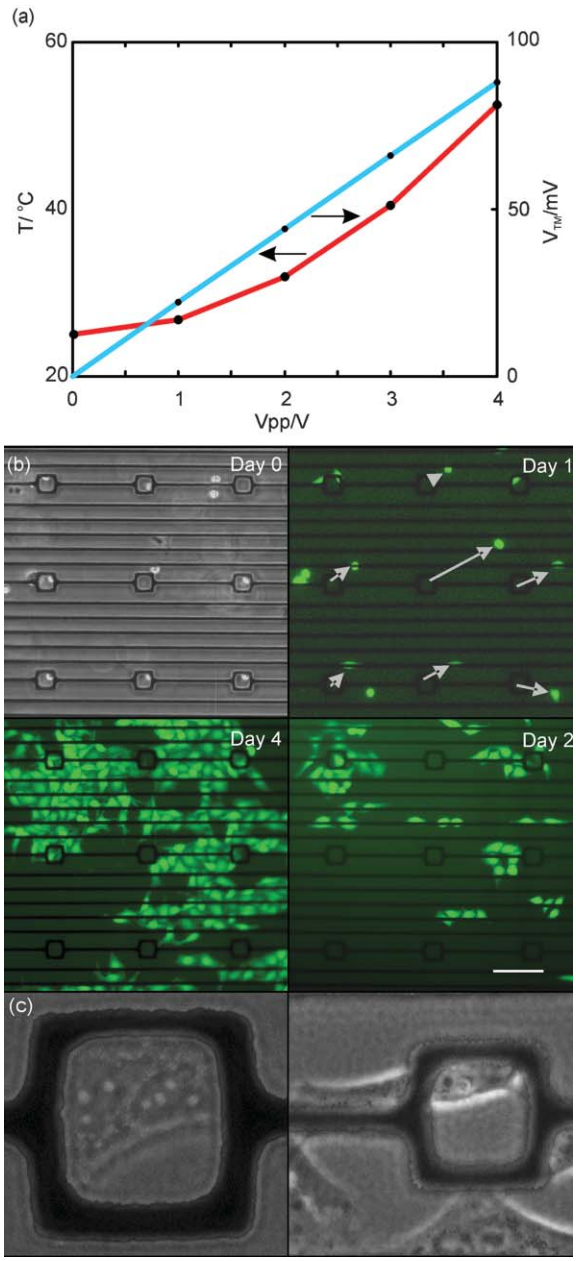

Fig. 4 Cell health. (a) Simulated temperature in the center of the trap (red line) and transmembrane voltages for trapped cells (blue line), for different peak voltages, at 10 MHz. Similar values were obtained for cells levitated above the IDEs. (b) Phase and fluorescent images of GFP-expressing HeLa cells trapped in a nDEP microwell array, showing that they exhibit normal morphology and proliferation over 4 days after being trapped at 1 V_{pp} and 10 MHz. Arrows in the Day 1 figure (top, right) show the displacement of cells that moved out of the trap. The scale bar represents 100 μm. (c) Phase images of single HeLa cells trapped in the nDEP microwells, showing that they exhibit normal morphology.

Simulations included conductive heat transfer and neglected convection, which is typically minimal in these systems (Péclet number, $Pe < 1$). We see that the temperature scales with the square of the applied voltage, as expected. Using a typical room temperature of 25 °C, we can avoid thermally stressing the cells by keeping the applied voltage to $\leqslant$2.5 V.

Modeling temperature rises in microsystems is often inaccurate because the exterior boundary conditions (between the device and ambient) are not known or well controlled. In our case, we set the exterior of the device to a fixed temperature boundary condition of room temperature. To determine whether this would result in realistic temperature modeling, we used a slightly different device where we fabricated an on-chip resistor specifically for measuring temperature (using the temperature coefficient of resistivity of Au). As seen in Fig. S4 (ESI†), the simulated and measured temperatures are comparable, validating our modeling approach. Thus, we believe that our thermal simulations are adequate design tools for avoiding thermal stresses.

Transmembrane potentials are the second way by which electric fields have been shown to affect cell physiology. When cells are placed in AC electric fields, an imposed AC voltage appears across the cell membrane. Since cells already maintain a constant (DC) transmembrane potential of $\sim$60 mV across their membrane, adding an additional potential could alter cell physiology.[27] For a spherical cell in a uniform electric field, the maximum imposed transmembrane potential is given by,[32]

$$V_{\mathrm{tm}} = \frac{1.5ER}{\sqrt{1+(\omega\tau)^2}}, \quad \tau = \frac{RC_{\mathrm{m}}\left(\rho_{\mathrm{cyto}} + 1/2\rho_{\mathrm{med}}\right)}{1+RG_{\mathrm{m}}\left(\rho_{\mathrm{cyto}} + 1/2\rho_{\mathrm{med}}\right)}$$

where E is the maximum electric field, R is the cell radius, ω is the frequency of the applied voltage, C_{m} is the capacitance of the cell membrane, ρ_{cyto} is the cytoplasmic conductivity, ρ_{med} is the conductivity of the medium, and G_{m} is the membrane conductivity for the cell. We see that the imposed transmembrane potential scales linearly with applied electric field and inversely with frequency above the critical frequency $1/\tau$. Thus, minimizing electric field intensity and increasing field frequency minimize V_{tm}.

We used our field modeling tools and the expression above to simulate the transmembrane potential experienced by cells due to the applied electric fields (Fig. 4(a)). As expected, the simulated transmembrane potential scales linearly with the applied voltage.

To use these simulations as a design tool, we must know the maximum potential that does not adversely affect cell health. Unfortunately, this value is not known, since the mechanism by which a rapidly oscillating potential affects cell physiology is not well understood. In addition, electric fields in DEP microsystems are necessarily non-uniform, which limits the accuracy of the simple V_{tm} expression above. Nonetheless, previous experimental[27,30] and theoretical[33] studies indicate that transmembrane voltages under 200 mV do not adversely affect cell physiology, and so we use this value as a rough reference point. As can be seen from Fig. 4(a), for our operating conditions ($\leqslant$2.5 V_{pp}, 10 MHz), the transmembrane potential does not exceed 50 mV.

In addition to voltage limitations imposed by cell health considerations, we also must deal with effects due to electrohydrodynamic (EHD) flows.[34] In our device EHD flows are exhibited primarily as convection of the media in the chamber. The media convects as a result of Joule heating caused by the ionic currents (details in the ESI†). We found that operation at voltages of 1–2 V_{pp} resulted in a slow accumulation of cells in the central region of the array due to this convective flow over the electrode array (ESI† Fig. S6). Once cells were bunched together, the problem of nonspecific adhesion of cells to the substrate was exacerbated, likely due to single stuck cells pulling others to the substrate. Thus, combining all the constraints, we chose an operation point of 1 V_{pp} and 10 MHz.

In Fig. 4(b) and (c) we show results of patterning HeLa cells, an adherent human tumor cell line. Again we see high patterning fidelity (Fig. 4(b)). More importantly, under these trapping conditions, we found that cells patterned on our array proliferated over 4 days and showed normal morphology (Fig. 4(c)). This demonstrates that our nDEP microwells can successfully be used to pattern multiple single cells in physiological media without grossly affecting cell health.

Manipulation of cells in our device

We have developed two modes of operation for our device (Fig. 5(a)). We use either pressure-driven flow alone, or a combination of pressure-driven flow and convective flow to move cells in the chamber. Using only pressure-driven flow, cells can be patterned more quickly (approximately 15 minutes). However, there is limited control over which nDEP microwells get filled. We can typically populate more than 70% of the nDEP microwells.

In the second mode (Fig. 5(b), ESI† video) we take advantage of the global electrohydrodynamic flows to obtain both linear (pressure-driven) and transverse (EHD) flows in our device. The pressure-driven flow was used to move cells along the array. On increasing the operating voltage to 2.5 V_{pp}, a significant EHD convective flow was set up in the flow chamber (ESI†) due to increased local Joule heating of the medium directly above the electrode array (by the ionic current). This flow pulled cells towards the center of the array. Cells will not get lifted by the flow unless they actually reach the center of the array, and the viscous drag force due to the EHD flow is greater than the gravitational force on the cell. In our experiments we did not observe this to happen. Upon decreasing the array voltage to 1 V_{pp} the convective flow stopped almost instantaneously. Using a combination of the two independent flows mentioned above, we were able to move cells into selected DEP microwells. We believe that this approach would be useful when the filling of adjacent sites in order to have a fixed intercellular distance is critical to a study, for example in studies of diffusible signaling and chemotactic responses.

Discussion

We have presented a method to build arrays of single cells using nDEP. The ability to pattern single cells is important for constructing and studying neuronal networks[10] and stem cell niches[11] *in vitro*.

In contrast to pDEP approaches that require cells to be suspended in special media, nDEP manipulation offers the advantage of allowing the cells to be in cell-culture media. Cells need to be in a medium with high salinity since they use an electrochemical gradient to obtain nutrients from their environment and to remove metabolites and ions from their cytosol. The sodium pump, also known as the

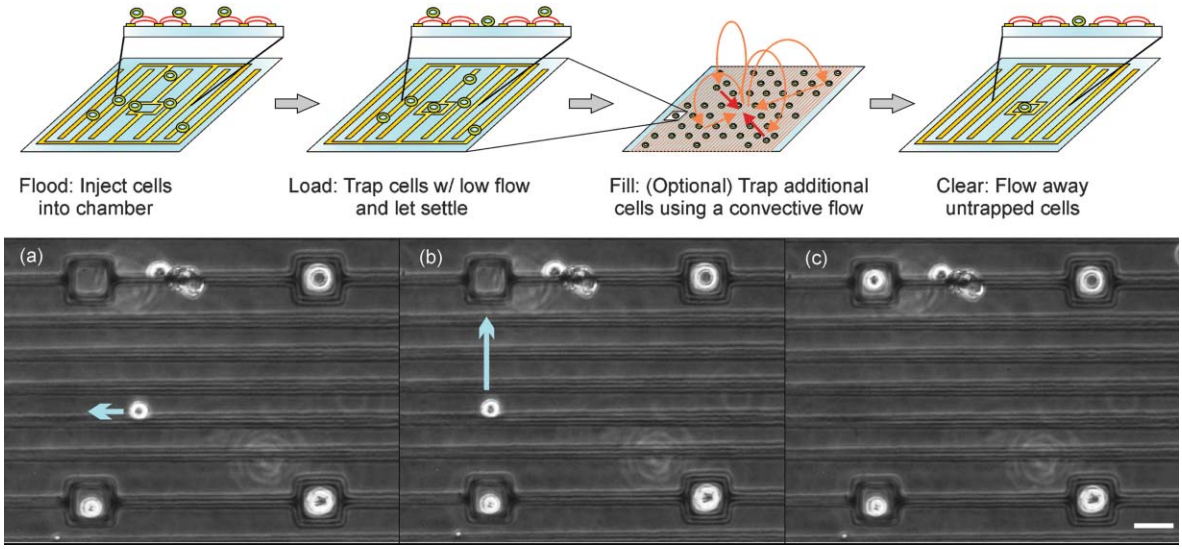

Fig. 5 Top: Schematic of operating procedure. We first inject cells into the chamber, with the electrodes on, at relatively high velocities of hundreds of microns per second. We then load cells into traps by flowing at very low speeds of around 1 μm s^{-1}. If required, we can then fill additional traps using EHD flows. In the 'Fill' step, orange lines show the motion of the fluid while red lines show the motion of (two) untrapped cells. The flow must be kept slow enough (<5 μm s^{-1}) so that cells do not get lifted with the flow. Finally, all untrapped cells are cleared from the array. Bottom: Use of convective flow to pattern cells. (a) → (b): Convective flow pushes untrapped cells towards the center of the electrode array (not shown at this scale) when electrodes are driven at 2.5 V_{pp}. Blue arrows show the movement of cells between frames. This flow is used to align cells with the trap. (b) → (c): Transition is made to pressure-driven flow using a syringe pump. All untrapped cells move in the same direction, along the array. The pressure-driven flow is used to push aligned cells into the traps. The scale bar represents 25 μm.

Na^+/K^+-ATPase, is responsible for establishing and maintaining this electrochemical gradient in animal cells, the driving force behind secondary transport systems.[35] The enzyme Na^+/K^+-ATPase is a component of the plasma membrane and transports Na^+ and K^+ using ATP hydrolysis. Thus, proper physiology demands that cells be in an environment with particular concentrations of these ions. Therefore cell-culture media for mammalian cells are designed to have similar ionic constituents as blood plasma, which results in an electrical conductivity of around 1.5 S m^{-1}. While many cell types can tolerate short exposures to low-conductivity media, it is commonly known that certain cell types do not fare well in such media. In these cases one must use physiological media. The high electrical conductivity (and higher permittivity) of physiological media make them more polarizable than cells at all frequencies; in this situation, only nDEP will occur.[28]

The conductivity of culture media is ~4 orders of magnitude larger than that of deionized (DI) water, and can result in significant Joule heating. Indeed, operating at electric fields in the 10^5 V m^{-1} range, as is routine in DEP microsystems, results in power densities of 10^{10} W m^{-3}. This can in turn result in significant temperature rises that can thermally shock cells.[36] The most common way to avoid this heating is to minimize the medium's electrical conductivity by substituting ions with a non-ionic solute (*e.g.*, sucrose) that provides osmotic balance without providing ions for electrical conduction. This medium has the advantage that it is ideally suited for pDEP cell manipulation, which is typically easier to accomplish than with nDEP. Indeed, single-cell trapping using pDEP was demonstrated by Suehiro and Pethig in 1998.[37] Subsequently, pDEP has been used by several groups to create arrays[7,17] and various biomimetic patterns of cells.[2,20] However, we can also exploit the small heating volume and large surface area for heat conduction in microsystems to minimize induced temperature rises. Coupling this favorable scaling with the nDEP microwell architecture results in a strong trap suitable for use in physiological media.

We have also engineered a unique fluidic manipulation method that uses convective flows in combination with pressure-driven linear flow, enabling two-dimensional manipulation of micron-sized objects. Although in our system, the flow is constrained toward the center of the array (*i.e.*, the hottest portion), one could conceivably create desired flow profiles by placing heating elements at specific locations on-chip. This convective flow could also be used to concentrate cells (ESI† Fig. S6). This would be useful for assays where only a small number of cells are available for patterning, such as when working with certain primary cells. The fluidics in our device provide for subsequent feeding or perfusion of cells. One could also, for example, flow in a second cell type after patterning the first one.

Although we have emphasized single-cell patterning in this work, our design could also be used to pattern other numbers of cells per site by increasing the size and changing the shape of the nDEP microwell. This would enable a study of the role of contact signaling with a precise number of neighboring cells.

Somewhat surprisingly, our trap strength is not limited by effects on cell physiology but by thermally induced EHD flows. Thus, if we could reduce heating in the device, we could increase our operating voltage and thus the trap strength. Since our goal is to use traditional cell culture media, lowering heating by lowering the conductivity of the medium is not a useful solution. An alternative way to decrease the temperature

rise is to increase the thermal conductivity of the substrate, since the temperature rise is directly related to the substrate thermal conductivity. For instance, fabricating our traps on a silicon wafer (thermal conductivity 150 W m^{-1} K^{-1} as compared to glass: 1.4 W m^{-1} K^{-1}) would allow us to increase the operating voltage to 10 V_{pp}, resulting in a significantly stronger trap, while still maintaining physiological temperatures and safe transmembrane potentials ($\sim$200 mV).

Materials and methods

Modeling

Modeling was performed using Matlab-based software developed in our lab[29] (free download available: http://www.rle.mit.edu/biomicro/publications.htm). Briefly, our software takes electric-field data and other experimental parameters and computes the total force on the particle everywhere in space. From this, streamlines are generated and used to determine the particles' trajectories. By varying fluid flow rates (and associated drag forces) we can determine the holding forces of particles in our systems. We extracted electric-field data from simulations using the commercial field solver Comsol Multiphysics (Comsol, Inc., Burlington, MA). Temperature modeling was also done using Comsol Multiphysics. After using the Electromagnetics module to determine the resistive heating in the flow chamber, we used the Heat Conduction module to determine the temperature at various locations on the device (details in ESI†). We determined the transmembrane potential using the maximum value of the electric field experienced by a trapped cell. For cell parameters, we used a radius of 5 μm, a membrane capacitance of 1.6 μF cm^{-2}, membrane conductivity of 0.22 S cm^{-2}, cytoplasmic conductivity of 0.75 S m^{-1} and cytoplasmic dielectric constant of 75. Medium conductivity is 1.5 S m^{-1} and dielectric constant is 80. These values are all taken from Huang *et al.*[38]

Temperature measurements

In order to validate our temperature modeling of cell health, we wanted to first match our model to some measured temperature values. Since thermocouples are incredibly large relative to a single DEP trap, they can only measure the average temperature across a large area of the chip. To obtain a more precise measurement of the temperature in the nDEP trap, we used a resistor-on-chip (ROC), placed between eight rows of twenty-four nDEP traps (ESI† Fig. S3). Since electrical resistance is a function of the resistor temperature, we can use the resistance value to determine temperature at the microscale level of the DEP trap. However, we must first calibrate the ROC to determine what the resistance values are at known temperatures. We placed the chip on a hotplate and measured the resistance for a range of temperatures. Since the temperature of the chip differed slightly from the temperature of the hotplate, we placed a thermocouple (HGKQIN-116, Omega, Stamford, CT) over the ROC and used this as the resistor temperature. We measured the temperature at five degree increments in the range of 25–60 °C, allowing us to generate a resistance *vs.* temperature curve.

We then measured resistance as a function of applied signal voltage, with a flow chamber over our ROC (ESI† Fig. S3). We flowed EtOH through the chamber at a low flow rate to remove any bubbles, using our fingers pressed against the flow chamber to apply pressure and keep a tight seal. We then flowed 1 mL of phosphate buffered saline (PBS) through the chamber to make sure all the EtOH was cleared away and then let the flow stabilize to zero. Then, at a frequency of 10 MHz, we applied a voltage of 0, 2.5, 3.5, 4.5, 5.5 V and recorded the ROC resistance.

Electrode traps

We designed the DEP microwells as square electrodes with an inner square side length of 25 μm, and two other line electrodes spaced 10 μm away. All electrode widths are 10 μm. The microwells are in a 10 × 10 square array, with a trap-to-trap distance of 200 μm. Between the DEP microwells we placed 3 other electrodes spaced by 30 μm each. These electrodes set up an interdigitated electrode array-like configuration (Fig. 2(a)).

We fabricated the electrodes by patterning gold onto Pyrex wafers. We cleaned wafers for 10 min in a Piranha solution (3 : 1 H_2SO_4 : H_2O_2), blew them dry with N_2, and then dehydrated them for 30 min at 225 °C. We then used the image-reversal photoresist Hoechst AZ-5214 (Celanese, Somerville, NJ) and photolithography to define the electrode patterns. Finally, we evaporated 10 nm of titanium and 200 nm of gold onto the slides followed by resist dissolution and metal liftoff in acetone.

Flow chamber and packaging

We created the flow chambers using a silicone gasket (19 × 6 × 0.5 mm; Grace Bio-Labs, Inc., Bend, OR). A piece of glass or a 4–5 mm thick sheet of baked polydimethylsiloxane (PDMS, Sylgard 184, Dow Corning, Midland, MI) was used to form the roof of the chamber. We drilled two holes in the glass lid to define inlet and outlet ports for the tubing. Alternatively, we cored two holes in the PDMS sheet using syringe needles (0.065″ outer diameter; Hamilton, Reno, Nevada). We then inserted polyetheretherketone (PEEK) tubing (Upchurch Scientific, Oak Harbor, WA) through these holes to provide fluidic access to the chamber, and applied epoxy to hold it in place. Finally, we clamped the chamber top and gasket to the bottom electrode slide using two binder clips for easy assembling and disassembling. The chamber was clamped at an angle to the electrode array to allow for loading with a lower density of cells (ESI† Fig. S8). Wires were electrically connected to the electrodes using conductive epoxy (Circuit Specialists, Mesa, AZ).

Fluidics

We connected the two inputs of a four-way valve (V-101D, Upchurch Scientific, Oak Harbor, WA) to a 3 mL syringe filled with cell suspension and a 5 mL syringe filled with medium. The 5 mL syringe was controlled using a syringe pump (KD Scientific 210C, Holliston, MA). One output on the four-way valve was connected to the flow chamber using polyethyleneteraphthalate (PET) tubing (0.03″ I.D., 0.048″

O.D.; Becton Dickinson and Co., Sparks, MD), and the other was connected to waste.

Cell culture

We cultured cells in 20 cm^2 dishes (Nunc, Rochester, NY). GFP-expressing HeLa cells (a generous gift from Dr Sangeeta Bhatia) were maintained in Dulbecco's Modified Eagle Medium (DMEM; Gibco, Grand Island, NY) supplemented with 10% fetal calf serum, 100 μg mL^{-1} penicillin, and 100 μg mL^{-1} streptomycin and incubated in 7.5% CO_2 at 37 °C. We passaged them at preconfluency no more than 25 times. HL60 cells (ATCC, Manassas, VA) were cultured in RPMI medium with additions as above. Prior to patterning experiments, we released cells into suspension and concentrated them to 10^6 cells mL^{-1}. HL60 cells were fluorescently labeled with chloromethylfluorescein diacetate (CMFDA; C2925, Molecular Probes, Eugene, OR; 20 μM, 30 minutes) for identification at (ex/em) 492/517 nm wavelengths.

Imaging

Images were taken on a Zeiss Axiovert 200 microscope (Carl Zeiss MicroImaging, Inc., Thornwood, NY) using a Spot RT Color camera (Diagnostic Instruments, Inc., Sterling Heights, MI). For fluorescence imaging we used a X-Cite 120 illumination system (Exfo Life Sciences, Ontario). Cell levitation heights were measured on a Zeiss Axioplan 2MOT microscope (Carl Zeiss MicroImaging, Inc., Thornwood, NY), by focusing alternately on cells and the substrate. We have previously verified that this method is accurate to within ~5 μm,[29] and was adequate for verifying that the levitation heights were in the 10–20 μm range.

Proliferation experiments

To demonstrate that cells patterned in our device are able to proliferate, we first patterned GFP-expressing HeLa cells in our device. After allowing the cells to attach for 30 minutes, we disconnected the patterning fluidics described above and attached a medium containing syringe to the fluidic input port of the device. Then we gently placed the device in a dish containing DMEM. The DMEM served to increase the local humidity in the dish and greatly reduce the rate of evaporation of medium from the device. We subsequently fed the cells once a day using the attached medium-containing syringe.

Cell adhesion force measurements

We used a parallel plate flow chamber (described above) measure the flow rate required to sweep away cells in contact with a glass substrate. The flow rate was controlled using a syringe pump (KD Scientific 210C, Holliston, MA). From the flow rate, we calculated the associated drag forces using our software (described above), which uses published analyses[39] to calculate the force on a stationary sphere near a surface in flow.

Electrical excitation

Sine wave excitation at 10 MHz was generated by an Agilent 33250A signal generator (Agilent, Palo Alto, CA). The signal was measured using a digital oscilloscope (Tektronix TDS 2024, Beaverton, OR).

Conclusions

We have presented a technique for accurately positioning single cells on a substrate using negative dielectrophoresis and cell–substrate adhesion. The cells are suspended in physiological media throughout the patterning process. We demonstrated that our device allows for the subsequent unrestricted spreading, movement, and proliferation of cells, enabling the study of these vital aspects of gross cell physiology. We show patterning results with both adherent (HeLa) and non-adherent (HL60) cell lines. We calculate the temperatures and transmembrane potential that cells in the device experience and compare them to physiologically acceptable levels described in previous studies. Finally, we have presented a new manipulation method that uses convective flows in combination with pressure-driven flows to achieve the two-dimensional positioning of cells. Thus, we have provided the foundation for an enabling technology that will allow the patterning of single cells in various configurations, allowing novel and detailed studies at the cellular scale, and reliable integration of cells into biosensors.

Acknowledgements

We would like to thank Dr Sangeeta Bhatia for providing us with the GFP-expressing HeLa cell-line we used in this study. We would also like to thank members of our group for their help and suggestions with experiments and this manuscript. This work was supported by the Singapore–MIT Alliance.

References

1 S. N. Bhatia, M. L. Yarmush and M. Toner, *J. Biomed. Mater. Res.*, 1997, **34**, 189.
2 D. R. Albrecht, G. H. Underhill, T. B. Wassermann, R. L. Sah and S. N. Bhatia, *Nat. Methods*, 2006, **3**, 369.
3 J. Fukuda, A. Khademhosseini, J. Yeh, G. Eng, J. J. Cheng, O. C. Farokhzad and R. Langer, *Biomaterials*, 2006, **27**, 1479.
4 Y. S. Zinchenko and R. N. Coger, *J. Biomed. Mater. Res., Part A*, 2005, **75**, 242.
5 P. Camelliti, A. D. McCulloch and P. Kohl, *Microsc. Microanal.*, 2005, **11**, 249.
6 M. Ozkan, T. Pisanic, J. Scheel, C. Barlow, S. Esener and S. N. Bhatia, *Langmuir*, 2003, **19**, 1532.
7 B. M. Taff and J. Voldman, *Anal. Chem.*, 2005, **77**, 7976.
8 J. J. Pancrazio, J. P. Whelan, D. A. Borkholder, W. Ma and D. A. Stenger, *Ann. Biomed. Eng.*, 1999, **27**, 697.
9 D. A. Stenger, G. W. Gross, E. W. Keefer, K. M. Shaffer, J. D. Andreadis, W. Ma and J. J. Pancrazio, *Trends Biotechnol.*, 2001, **19**, 304.
10 M. A. Colicos and N. I. Syed, *J. Exp. Biol.*, 2006, **209**, 2312.
11 E. Fuchs, T. Tumbar and G. Guasch, *Cell*, 2004, **116**, 769.
12 D. Falconnet, A. Koenig, T. Assi and M. Textor, *Adv. Funct. Mater.*, 2004, **14**, 749.
13 C. S. Chen, M. Mrksich, S. Huang, G. M. Whitesides and D. E. Ingber, *Science*, 1997, **276**, 1425.
14 N. M. Toriello, E. S. Douglas and R. A. Mathies, *Anal. Chem.*, 2005, **77**, 6935.
15 A. Revzin, R. G. Tompkins and M. Toner, *Langmuir*, 2003, **19**, 9855.
16 D. Di Carlo, N. Aghdam and L. P. Lee, *Anal. Chem.*, 2006, **78**, 4925.

17 D. S. Gray, J. L. Tan, J. Voldman and C. S. Chen, *Biosens. Bioelectron.*, 2004, **19**, 1763.
18 P. Y. Chiou, A. T. Ohta and M. C. Wu, *Nature*, 2005, **436**, 370.
19 A. Sebastian, A. M. Buckle and G. H. Markx, *J. Micromech. Microeng.*, 2006, **16**, 1769.
20 C. T. Ho, R. Z. Lin, W. Y. Chang, H. Y. Chang and C. H. Liu, *Lab Chip*, 2006, **6**, 724.
21 J. Voldman, M. L. Gray, M. Toner and M. A. Schmidt, *Anal. Chem.*, 2002, **74**, 3984.
22 M. Frenea, S. P. Faure, B. Le Pioufle, P. Coquet and H. Fujita, *Mater. Sci. Eng., C*, 2003, **23**, 597.
23 Z. Yu, G. X. Xiang, L. B. Pan, L. H. Huang, Z. Y. Yu, W. L. Xing and J. Cheng, *Biomed. Microdev.*, 2004, **6**, 311.
24 J. Voldman, *Annu. Rev. Biomed. Eng.*, 2006, **8**, 425.
25 M. M. Stevens, M. Mayer, D. G. Anderson, D. B. Weibel, G. M. Whitesides and R. Langer, *Biomaterials*, 2005, **26**, 7636.
26 J. A. Barron, P. Wu, H. D. Ladouceur and B. R. Ringeisen, *Biomed. Microdev.*, 2004, **6**, 139.
27 T. Muller, A. Pfennig, P. Klein, G. Gradl, M. Jager and T. Schnelle, *IEEE Eng. Med. Biol. Mag.*, 2003, **22**, 51.
28 T. Schnelle, T. Muller, A. Voigt, K. Reimer, B. Wagner and G. Fuhr, *Langmuir*, 1996, **12**, 801.
29 A. Rosenthal and J. Voldman, *Biophys. J.*, 2005, **88**, 2193.
30 T. Heida, J. B. M. Wagenaar, W. L. C. Rutten and E. Marani, *IEEE Trans. Biomed. Eng.*, 2002, **49**, 1195.
31 S. J. Beebe, P. M. Fox, L. J. Rec, K. Somers, R. H. Stark and K. H. Schoenbach, *IEEE Trans. Plasma Sci.*, 2002, **30**, 286.
32 E. Neumann, A. E. Sowers and C. A. Jordan, *Electroporation and electrofusion in cell biology*, Plenum Press, New York, 1989.
33 P. T. Vernier, M. J. Ziegler, Y. H. Sun, W. V. Chang, M. A. Gundersen and D. P. Tieleman, *J. Am. Chem. Soc.*, 2006, **128**, 6288.
34 A. Castellanos, A. Ramos, A. Gonzalez, N. G. Green and H. Morgan, *J. Phys. D: Appl. Phys.*, 2003, **36**, 2584.
35 G. Scheiner-Bobis, *Eur. J. Biochem.*, 2002, **269**, 2424.
36 S. Lindquist, *Annu. Rev. Biochem.*, 1986, **55**, 1151.
37 J. Suehiro and R. Pethig, *J. Phys. D: Appl. Phys.*, 1998, **31**, 3298.
38 Y. Huang, X. B. Wang, F. F. Becker and P. R. C. Gascoyne, *Biophys. J.*, 1997, **73**, 1118.
39 A. Goldman, R. Cox and H. Brenner, *Chem. Eng. Sci.*, 1967, **22**, 653.